

Critical Temperature Dependence of Heterodyne Mixing in Superconducting Nb based Hot-Electron Bolometers

I. Siddiqi and D.E. Prober

Department of Applied Physics, Yale University, 15 Prospect Street, New Haven, Connecticut 06520-8284

B. Bumble and H.G. LeDuc

Center for Space Microelectronics Technology, Jet Propulsion Laboratory, Caltech, Pasadena, California 91109

Nb hot-electron bolometers (HEBs) with critical temperature $T_c = 5$ to 6 K have previously demonstrated good heterodyne mixing performance at THz frequencies. HEBs with a lower critical temperature are predicted to have improved performance with lower noise. We present microwave (30GHz) mixing measurements on Nb HEB mixers with T_c between 1.4 and 5.3 K. The reduced T_c is obtained by application of a magnetic field, or by use of a bi-layer microbridge of Nb and Au with $T_c = 1.6$ K. The mixer output noise and voltage range of low mixer noise are observed to decrease approximately linearly with reduction of T_c . The Nb-Au mixer has a mixer noise temperature $\bar{T}_M = 50$ K (DSB) with reasonable dynamic range, and thus is promising for future single pixel and array receivers for THz spectroscopy.

Heterodyne spectroscopy at terahertz frequencies is a sensitive tool for identifying molecular species important in star formation and in atmospheric chemistry processes.¹ Hot-electron bolometer (HEB) mixers are well suited for such spaceborne and ground-based astronomical applications. Unlike superconductor-insulator-superconductor (SIS) mixers, the HEB is not limited by the superconducting energy gap frequency and can operate at several terahertz.^{2,3} Also, diffusion-cooled HEB mixers can have very large intermediate frequency (IF) bandwidths; up to 9 GHz has been demonstrated.⁴ HEB mixers are considerably more sensitive than Schottky diode mixers, which have been used for higher frequency applications where SIS mixers are limited by the gap frequency or by RF losses.

The HEB mixer consists of a narrow, thin superconducting microbridge contacted with thick normal-metal films; see

Fig. 1. The microbridge operates in the resistive state, due to application of local oscillator (LO) power and DC bias. When the RF signal is applied, the electron temperature of the microbridge (and thus the device resistance) oscillates at the IF. The IF bandwidth is determined by the inverse of the thermal relaxation time for cooling the hot electrons in the microbridge.^{5,6} Diffusion-cooled Nb mixers use hot-electron out-diffusion for cooling.⁶ These have demonstrated very low noise at 2.5 THz with receiver noise temperature $T_R = 1800$ K (DSB).⁴ The mixer noise temperature T_M is estimated to be 350 K (DSB) for a similar device measured also at 2.5 THz.⁷ NbN phonon-cooled mixers also have good performance.^{3,8}

Diffusion-cooled HEB mixers consisting of a superconductor with lower critical temperature (T_c) are predicted to have improved performance.^{9,10} In optimized HEBs, thermal fluctuation noise is

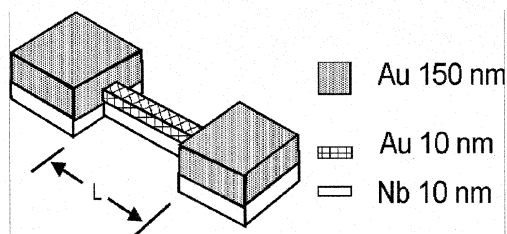


Figure 1: Superconducting mixer geometry for the Nb-Au HEB, device B. The thin layer of Au above the Nb lowers the T_c of the microbridge. The Nb HEB mixer, device A, has no gold layer on top of the microbridge.

the dominant noise source neglecting quantum effects. In this case, T_M is predicted to decrease linearly with T_c .¹¹ Another advantage of lowering the microbridge T_c is that the required LO power decreases. The LO power for a diffusion cooled mixer is predicted to be¹² $P_{LO} \approx (4\mathcal{L}/R) (T_c^2 - T^2)$, where $\mathcal{L} = 2.45 \times 10^{-8} \text{ W}\cdot\Omega/\text{K}^2$ is the Lorenz constant, R is the electrical resistance, and T is the temperature of the normal banks. For optimum performance one has $T \ll T_c$, and thus $P_{LO} \propto T_c^2$, being in the range 1 – 30 nW. Since output power from solid state LO sources at terahertz frequencies may be limited to μW , a mixer with a small required P_{LO} is desired, especially for space-borne missions and large format arrays.

A HEB mixer with reduced T_c should have improved performance, but will also be more susceptible to saturation effects that degrade T_M . Such effects can be important in a THz receiver but are negligible in the microwave measurements. T_M is given by $T_M (\text{DSB}) = T_{\text{out}} / 2\eta$, with η the conversion efficiency and T_{out} the output noise temperature. T_M is minimum only over a finite voltage range but then in-

creases due to the decrease of η . Input saturation will occur when the absorbed RF background power is $\sim 0.2 P_{LO}$, as this reduces η .^{13,14} Output saturation is due to RF background power downconverted to the IF which causes the voltage to deviate far from the optimum bias voltage. We characterize the voltage range for which T_M remains within a factor of two of its lowest value as ΔV_{opt} . Simulations we have conducted¹³ using a discretized model for the microbridge¹⁵ suggest that ΔV_{opt} will scale approximately linearly with T_c , for the simple case where the contacts to the microbridge do not perturb the superconductivity in the microbridge. This is the case for Nb devices. (In the case of Al HEBs,^{13,16,17} the voltage range is further reduced due to contact effects.) The value \bar{T}_M we report in the Table and Fig. 3 below is an average of T_M over the 20 μV interval of bias voltage for which this average is lowest. This definition provides a more realistic value of the expected mixer noise temperature in a receiver where averaging due to background noise or bias variations might be present.

We report here on two Nb HEBs. The first, a Nb HEB, device A, was fabricated at JPL. Similar devices were previously measured in zero magnetic field at 20, 600, 1200, and 2500 GHz.^{4,7,18-20} The dimensions are 0.08 μm wide, 10 nm thick, and length $L = 0.24 \mu\text{m}$. T_c in zero field is 5.3 K and is reduced to 1.4 K by applying a perpendicular magnetic field. The IF bandwidth is 1.4 GHz. The Nb-Au HEB, device B, was fabricated at Yale using double angle deposition.²¹ A thin bilayer resist is used as the liftoff stencil. A thin (10 nm) Nb film is first sputter deposited at normal incidence, followed by Au which is sputter deposited at a 45 degree angle. A thick layer of gold deposits on the contacts, mak-

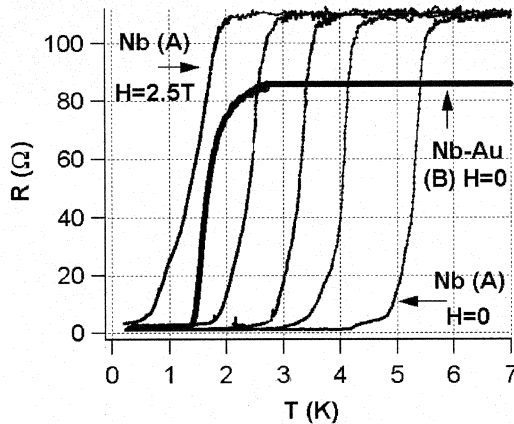


Figure 2: Resistance vs. temperature curves for the Nb HEB, device A, with $H=0, 1, 1.5, 2, 2.5$ T and the Nb-Au HEB, device B, in zero magnetic field.

ing them non-superconducting, and a thin layer of Au (about 10 nm) deposits on top of the Nb microbridge, lowering its T_c . The Nb-Au HEB is $0.20 \mu\text{m}$ wide and $L = 0.48 \mu\text{m}$. T_c in zero applied magnetic field is 1.6 K. The measured IF bandwidth is 1.2 GHz, consistent with that predicted from the length and diffusion constant (determined from H_{c2}). $R(T)$ curves are given in Fig. 2 for the Nb HEB, device A, in various magnetic fields and for the Nb-Au HEB in zero field, device B. A third device, a Nb HEB was also studied. Some of its properties were previously reported.¹⁴ It followed the trends of device A. However, it displayed a two-step transition in zero field, which broadened dramatically with application of a field. Its noise was about twice that of the Nb HEB, device A, which we ascribe to the unusual transition shape. We therefore do not list that device. The measurements use a liquid ^3He cryostat equipped for microwave mixing measurements up to 40 GHz, at $T = 0.2$ K. Temperatures up to $(1/2)T_c$ could be used without significant performance degradation. For each value

of T_c , the LO power and DC power is adjusted to optimize for the conversion efficiency. Microwave measurements are employed for their rapid turnaround, low background noise, and ease of calibration. Past studies of Nb devices¹⁸ showed reasonable correlation between such microwave measurements and THz mixing results. A summary of the device parameters is presented in the Table. T_{out} and η are measured at 1.4 GHz, and values listed in Table I are those extrapolated to $\text{IF} = 0$ using the established frequency dependence. The values of \bar{T}_M in the Table and Fig. 3 are at $\text{IF} = 1.4$ GHz.

Achieving low mixer noise is the key. The minimum \bar{T}_M for both devices is given as a function of T_c in Fig. 3. For device A, \bar{T}_M decreases linearly with the reduction of T_c , down to $T_c \sim 3$ K, and then increases for lower values of T_c . The decrease of \bar{T}_M with reduction of T_c is consistent with theoretical expectations, and results simply from the reduction of thermal fluctuations if η is independent of T_c . Specifically, the theory in Ref. 11 predicts $T_M \sim T_c$ when operating with very small conversion loss and thermal fluctuations dominating all other noise processes. We observe a linear decrease in mixer noise temperature with T_c , as predicted, but with larger conversion loss (maximum conversion efficiency $\eta = -11$ dB). The reason for the increase of T_M for device A for $T_c < 3.3$ K is the reduction of η for applied fields of 2 and 2.5 T, for $T_c = 2.4$ and 1.4 K respectively (see Table). This reduction of η likely results from the very small critical currents obtained at the largest fields ($0.5 \mu\text{A}$ at 2.5 T), indicating non-uniform superconductivity occurs at the largest fields. This can be seen in Fig 2, where the resistive transitions at 2 and 2.5 T are seen to

Table I: Nb HEB mixer parameters. The conversion efficiency and output noise reported are IF=0 values. The \bar{T}_M listed is the minimum averaged over 20 μ V, as also in Fig. 4.

Device	T_c (K)	H (T)	$I_c(0)$ (μ A)	T_{output} (K)	η (dB)	\bar{T}_M (K)	ΔV_{opt} (μ V)
(A) Nb	5.3	0	100	26	-11	170	200
	4.0	1.0	13	16	-11	110	135
	3.3	1.5	7	14	-11	95	130
	2.4	2.0	4	10	-15	180	90
	1.4	2.5	0.5	4	-20	250	40
(B) Nb-Au	1.6	0	14	3	-12.5	50	130

have very large fractional temperature widths. The small critical current at 2.5 T of device A, 0.5 μ A, can be compared with the critical current of the Nb-Au device which has a similar T_c , for which $I_c = 14 \mu$ A. For the Nb-Au HEB, larger conversion efficiency results and $\bar{T}_M = 50$ K. P_{LO} for the Nb-Au HEB is 2 nW compared to 0.4nW for device A at $T_c = 1.4$ K. The resistive transition of this Nb-Au device, in Fig. 2, is more uniform and narrower than device A at 2.5 T. We believe that the relatively large critical current, low mixer noise, $\bar{T}_M = 50$ K (DSB), and relatively good conversion efficiency ($\eta = -12.5$ db) are characteristic of a reduced- T_c device with a sharp transition. Another Nb-Au device has similar properties to device B.

For a practical mixer, low noise operation must be achievable over a reasonable operating range. The IV curve

and T_M as a function of bias voltage are shown for the Nb-Au, device B, in Fig. 4. The IV curves are for $P_{\text{LO}} = 0$ and for $P_{\text{LO}} = 2$ nW, the absorbed power which gives the

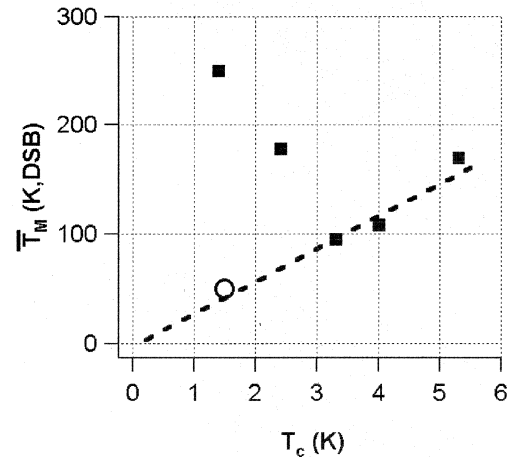


Figure 3: Mixer noise temperature from Table I for devices A (squares) and B (circle) as a function of T_c . $T_{\text{bath}} = 0.2$ K. The dashed line is the expected linear decrease in noise temperature resulting from a decrease in thermal fluctuations.

minimum value of T_M . The critical current when increasing the voltage is $14 \mu\text{A}$; small thermal hysteresis is seen in Fig. 4. The minimum $T_M = 45 \text{ K}$, occurs just above $150 \mu\text{V}$. We show data for T_M only for those voltages for which operation is completely stable. T_M remains below 90 K for voltages between 150 and $280 \mu\text{V}$, giving a voltage range $\Delta V_{\text{opt}} = 130 \mu\text{V}$. For P_{LO} between 2 and 4 nW , the minimum T_M remains below 50 K . For P_{LO} between 1 and 7 nW , $T_M < 100 \text{ K}$. Thus, for array applications, small variations in the optimum P_{LO} for each element due to fabrication imperfections or pixel-to-pixel differences in the coupled P_{LO} should not result in a significant change in the noise temperature of each pixel. We list ΔV_{opt} and other microwave parameters for both devices at all fields in the Table. We see in the Table that ΔV_{opt} decreases approximately linearly with reduction of T_c for the Nb HEB.

We finally consider saturation issues. For Device A, ΔV_{opt} scales approximately linearly with T_c , as shown in the Table, in good agreement with numerical calculations.¹⁴ These predict $\Delta V_{\text{opt}} \sim 100 \mu\text{V}$ for a HEB with a uniform $T_c = 1.6 \text{ K}$ along the length of the bridge. With the experimental value $\Delta V_{\text{opt}} \sim 130 \mu\text{V}$, we estimate for the Nb-Au HEB the level of IF power which would begin to produce output saturation as approximately 40 pW at the IF. This corresponds to a background noise temperature $T_{\text{back}} = 13,000 \text{ K}$ with an IF bandwidth of 2 GHz , assuming $\eta = -12.5 \text{ db}$ (total RF bandwidth of 4 GHz due to both sidebands). Such a large level of background noise is not expected in typical applications.²² Input saturation would result if the coupled broadband background noise power is comparable to $P_{\text{LO}} = 2 \text{ nW}$. For receivers with 200 GHz RF bandwidth, the

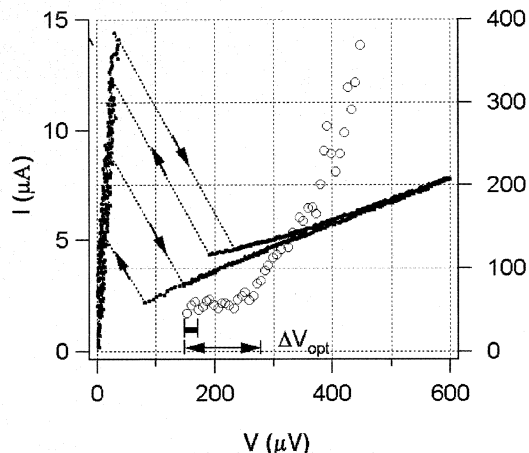


Figure 4: Mixer noise temperature and conversion efficiency for the Nb-Au HEB, device B, as a function of bias voltage. T_M is the mixer noise temperature at that voltage. The heavy bar shows the 20 mV range over which the average of T_M (\bar{T}_M) is found.

incident background power is 0.5 nW for $T_{\text{back}} = 200 \text{ K}$. The Nb-Au HEB should thus show no significant saturation effects. Overall, the Nb-Au HEB shows better performance than a Nb HEB in a magnetic field. In applications where the instantaneous RF bandwidth is very large ($\geq 0.5 \text{ THz}$), Nb-Au devices with slightly higher T_c , for increased P_{LO} , can be used to avoid input saturation. Such devices can be produced with a thinner Au layer. Thus, the Nb-Au HEB looks very promising for THz applications with low mixer noise and very small required LO power, and should provide sufficient dynamic range for the anticipated applications.

We thank C.M. Wilson for assistance with metal deposition in the Nb-Au device fabrication, and B.S. Karasik and W.R. McGrath for useful discussions. This research was supported by the NSF AST 9618705 and the NASA Office of Space Science. Funding for I.S. was provided in part by a NASA Graduate Student Fellowship.

¹ T.G. Phillips and J. Keene, Proc. IEEE **80**, 1662 (1992).

² W.R. McGrath, B.S. Karasik, A. Skalare, R. Wyss, B. Bumble, and H.G. LeDuc, Proc. of the SPIE **3617**, (1999).

- ³ A.D. Semenov, H-W. Hubers, J. Schubert, G. N. Gol'tsman, A. I. Elantiev, B. M. Voronov, and E. M. Gershenzon, *J. Appl. Phys.* **88**, 6758 (2000).
- ⁴ R. A. Wyss, B.S. Karasik, W.R. McGrath, B. Bumble, and H.G. LeDuc, in *Proceedings of the 10th International Symposium on Space Terahertz Technology*, edited by T. Crowe and R.M. Weikle (University of Virginia, Charlottesville, VA, 1999), pp. 215-228.
- ⁵ E. M. Gershenzon, G.N. Gol'tsman, I.G. Gogidze, Y.P. Gusev, A.I. Elantiev, B.S. Karasik, and A.D. Semenov, *Superconductivity* **3**, 1582 (1990).
- ⁶ D.E. Prober, *Appl. Phys. Lett.* **62**, 2119 (1993).
- ⁷ B.S. Karasik, M.C. Gaidis, W.R. McGrath, B. Bumble, and H.G. LeDuc, *Appl. Phys. Lett.* **71**, 1567 (1997).
- ⁸ E. Gerecht et al., in *Proceedings of the 11th International Symposium on Space Terahertz Technology*, edited by J. East (University of Michigan, Ann Arbor, MI, 2000), pp. 209-218.
- ⁹ B.S. Karasik and W.R. McGrath, in *Proceedings of the 9th International Symposium on Space Terahertz Technology*, edited by W.R. McGrath (Pasadena, CA, 1998), pp. 73-80.
- ¹⁰ It is unclear if superconducting films are available to produce phonon-cooled mixers with lower T_c , but also having adequate IF bandwidth. If such materials can be found, our arguments for reduction of T_c would also apply to these phonon-cooled devices.)
- ¹¹ B.S. Karasik and A.I. Elantiev, *Appl. Phys. Lett.* **68**, 853 (1996); the quantum mixer noise is $T_M^Q = \hbar v/k = 48K * f(\text{THz})$ and is negligible in the microwave experiments. HEB mixers are not yet quantum-limited in noise performance, and a decrease in noise temperature is thus predicted for devices with lower T_c , even when operating at THz frequencies where T_M^Q is larger than at 30 GHz.
- ¹² P.J. Burke, Ph.D. thesis, Yale University, 1997, available from authors.
- ¹³ I. Siddiqi, A. Verevkin, R. Jahn, D.E. Prober, A. Skalare, W.R. McGrath, P.M. Echternach, and H.G. LeDuc, submitted to *J. Appl. Phys.* (7/2000).
- ¹⁴ I. Siddiqi, D.E. Prober, B. Bumble, and H.G. LeDuc, in *Proceedings of the 12th International Symposium on Space Terahertz Technology*, edited by I. Mehdi (San Diego, CA, 2001), to be published.
- ¹⁵ A. Skalare and W.R. McGrath, *IEEE Trans. Appl. Supercond.* **9**, 4444 (1999).
- ¹⁶ I. Siddiqi, A. Verevkin, D.E. Prober, A. Skalare, W.R. McGrath, P.M. Echternach, and H.G. LeDuc, *IEEE Trans. Appl. Supercond.* **11**, 958 (2001).
- ¹⁷ A. Skalare, W.R. McGrath, P.M. Echternach, H.G. LeDuc, I. Siddiqi, A. Verevkin, and D.E. Prober, *IEEE Trans. Appl. Supercond.* **11**, 641 (2001).
- ¹⁸ P.J. Burke, R.J. Schoelkopf, D.E. Prober, A. Skalare, B.S. Karasik, M.C. Gaidis, W.R. McGrath, B. Bumble, and H.G. LeDuc, *J. Appl. Phys.* **85**, 1644 (1999).
- ¹⁹ A. Skalare, W.R. McGrath, B. Bumble, H.G. LeDuc, P.J. Burke, A.A. Verheijen, and D.E. Prober, *IEEE Trans. Appl. Supercond.* **5**, 2236 (1995).
- ²⁰ A. Skalare, W.R. McGrath, B. Bumble, and H.G. LeDuc, *IEEE Trans. Appl. Supercond.* **7**, 3568 (1997).
- ²¹ P.M. Echternach, H.G. LeDuc, A. Skalare, and W.R. McGrath, in *Proceedings of the 10th International Symposium on Space Terahertz Technology*, edited by T. Crowe and R.M. Weikle (University of Virginia, Charlottesville, VA, 1999), pp. 261-268.
- ²² In contrast to these results for Nb and Nb-Au, we find for Al HEBs that output saturation at the IF is a significant issue. A large fraction of the microbridge (up to 50%) is made non-superconducting even at $T = 0$ by the normal contacts, so that $\Delta V_{\text{opt}} < 10 \mu\text{V}$ for a typical Al HEB. This is consistent with our simulations.